

# Results from a "Small Box" Real-Time Molecular Contamination Monitor on STS-3

J. Triolo,\* R. Kruger,† and R. McIntosh‡

*NASA Goddard Space Flight Center, Greenbelt, Maryland*

C. Maag‡

*Jet Propulsion Laboratory, Pasadena, California*  
and

P.A. Porzio§

*U.S. Air Force, Los Angeles, California*

A small, contamination monitor package (CMP), instrumented with four temperature-controlled quartz crystal microbalances (TQCM) was flown on STS-3 as part of the first flight package of the Office of Space Science (OSS-1) payload. The microbalances were located at the surfaces of a small box mounted to the rear and port side of the OSS-1 payload pallet, approximately 12.6 m (41.2 ft) aft of the forward bulkhead, 1.8 m (6.0 ft) towards the port side from the centerline, and 0.3 m (0.9 ft) above the sill. The sensing surfaces of the microbalances faced (relative to the Orbiter cargo bay) port, starboard, out, and aft pointed down at 45 deg into the bay. The data indicate a strong dependence on the temperature of the cargo bay which, in turn, depends on the Orbiter attitude towards the sun. In the tail-to-sun position, accretion rates on 0°C TQCM surfaces began as high as 100 ng cm<sup>-2</sup> h<sup>-1</sup> during the first hour, but fell rapidly to a few ng cm<sup>-2</sup> h<sup>-1</sup> (both positive and negative) almost immediately thereafter. These low rates existed even when the TQCMs were set to -30°C as the cargo bay continued cooling. Measurements made in the nose-to-sun attitude (a slightly warmer attitude) showed the same low rates at 20 and -30°C. In the bay-to-sun attitude, accretion rates (R) began rising to near 100 ng cm<sup>-2</sup> h<sup>-1</sup> for the aft facing sensor at 0°C. The others indicated rates in the vicinity of 20 ng cm<sup>-2</sup> h<sup>-1</sup>. At 20°C, all microbalances indicated accretions in the vicinity of 20 ng cm<sup>-2</sup> h<sup>-1</sup>.

## Introduction

**E**VEN before the Induced Environment Contamination Monitor (IECM)<sup>1</sup> was first flown on the second Space Transportation System (STS-2), it was recognized that a small-box contamination monitor was needed to characterize the environment induced not only by the Orbiter but also by the varying cargo mixes beyond the limited number of scheduled IECM flights. From early estimates of the Shuttle-induced environment and molecular outgassing flux measured during thermal vacuum test, Scialdone<sup>2</sup> concluded that in the vicinity of the cargo, the cargo would have the largest influence on the environment. Also, as a contamination management device, real-time monitors can indicate safe operational periods for sensitive, attached payloads. With these common interests, Goddard Space Flight Center (GSFC), the California Institute of Technology, Jet Propulsion Laboratory (JPL), and the United States Air Force Space Division (SD) collaborated to develop the Contamination Monitor Package (CMP). The CMP contained the quartz crystal microbalances of this report, and was seen as a forerunner of an operations monitor. The opportunity to participate in this program came late and led to the decision to go ahead with an imperfect CMP. This will be discussed more fully later.

## Description of Instrument

As it was a latecomer to the program, the locations on the OSS-1 pallet available for the CMP were extremely limited. The position selected was on the aft end of shelf 6 (Fig. 1). The OSS-1 pallet was well aft in the cargo bay, one bay (approximately 3 m) forward of the Development Flight Instrumentation (DFI) on which the IECM was mounted. The DFI was at the aftmost position. In terms of STS coordinates, the CMP was located approximately at  $x=1070$ ,  $y=-72$ , and  $z=421$ .

The CMP is shown in Fig. 2. It was approximately 20 cm high, 18 cm wide, and 30 cm long (8 × 7 × 12 in.) and weighed about 7 kg (15 lb). The average power consumption was about 7 W. The box itself was passively thermally controlled using silver teflon for radiating surfaces and aluminized Kapton multilayer insulation for radiation insulation. Thermal conductances to the OSS-1 pallet were minimized.

The CMP instruments included two passively controlled witness samples (which will not be discussed here) supplied by the Naval Research Laboratory and four actively controlled TQCMs. The basic TQCM configuration was similar to those of the IECM<sup>1</sup> except that the temperature could be controlled from the ground. The use of thermoelectrics in a TQCM is described in Ref. 3. Reference 4 is an early reference to the use of the quartz crystal microbalance in space for the measurement of contaminants.

The TQCM temperatures could be varied from -60 to +80°C. This control was exercised by telemetry from the ground without crew involvement. The data was recorded on the OSS-1 tape recorder for later playback on the ground, recorded on the Orbiter tape recorder for playback from orbit, and was telemetered in real-time during passes over ground stations.

The orientation of the four TQCMs is shown in Fig. 2. TQCM 1 faced aft and pointed down into the payload bay at an angle of 45 deg. TQCM 2 faced to port. TQCM 3 faced out of the payload bay, and TQCM 4 faced to starboard.

Presented as Paper 83-0251 at the AIAA 21st Aerospace Sciences Meeting, Reno, Nev., Jan. 10-13, 1983; received July 1, 1983; revision received Feb. 13, 1984. This paper is declared a work of the U.S. Government and therefore is in the public domain.

\*Aerospace Technologist, Thermal Engineering Branch. Member AIAA.

†Aerospace Technologist, Thermal Engineering Branch.

‡Group Supervisor, Contamination Control and Management.

§Captain, USAF, Space Division; presently, NASA Headquarters, Washington, D.C.

The TQCMs have a sensitivity of  $1.56 \times 10^{-9} \text{ g cm}^{-2} \text{ Hz}^{-1}$ . While the more basic unit of measure for the TQCM is a surface loading density ( $\text{g cm}^{-2}$ ), some results will be expressed in terms of nm/10 (or Angstrom units) of thickness, assuming a contaminant density of  $1.0 \text{ g cm}^{-3}$ .

The TQCMs incorporated in the CMP were procured from Faraday Laboratories. Figure 3 schematically represents a typical TQCM. The sensor consisted of a matched pair of quartz crystals, each resonated at approximately 15 MHz. The crystals were designated as a sensor (which faced the environment) and reference crystal (protected from the environment). The sensing crystal was displaced in frequency approximately 1 kHz below the reference crystal. The crystals were optically polished and coated with aluminum. Only the TQCM 1 sensor crystal was overcoated with magnesium fluoride ( $\text{MgF}_2$ ) to simulate a typical optical reflective element; the other crystals had no coating placed over the evaporated aluminum sensor surface. The output of a mixer circuit provided a frequency which increased when the mass on the sensing crystal increased. In addition, a two-stage thermoelectric device was located directly behind the crystals to provide for cooling or heating of the quartz crystals.

Within the CMP box, the electronics module occupied a major part of the volume (Fig. 2). The flight electronics CMP included the command decoder, telemetry (data) generator/interface, and proportional temperature controllers for the TQCMs.

Commands received through the OSS-1 command system provided the capability to turn each TQCM on or off and to set its temperature to any integer value between  $-60$  and  $+80^\circ\text{C}$ . Once commanded, the proportional controllers would maintain a TQCM, at the specified temperature until commanded to another setpoint. Wherever possible, complementary metal oxide semiconductor logic was used to minimize power and energy requirements. The proportional controllers utilized a switching power supply design which incorporated pulse frequency and pulse width modulation

techniques to minimize the power required to control the thermoelectric coolers of the TQCM. This approach provided a dc signal to the thermoelectric devices without the low efficiency encountered with unswitched dc power supplies.

Data were generated by the CMP electronics for monitoring TQCM and heat sink temperatures through calibrated bridge networks; two precise voltage measurements were used to calibrate the telemetry system. Digital data also represented the TQCM frequencies and status information. The TQCM frequencies were resolved within 1 Hz with a maximum reading capability of 65,535 Hz. A unique synchronization pattern provided for the stripping of the CMP data from the overall OSS-1 data stream. CMP data were obtained approximately every 1.64 s.

Telemetered data were processed through the NASA Johnson Space Center and OSS-1 computers and issued as an RS232C compatible signal. This signal was processed through a small digital computer system for display in engineering units on a cathode ray tube display and printer.

The TQCM crystals were cut to minimize temperature sensitivity and were paired to decrease the temperature effects. Because of the limitations, no preflight temperature calibrations were conducted; post-flight calibration was carried out by Faraday Labs on each sensor over the entire temperature range experienced in flight. Also, a solar simulator was used to demonstrate the magnitude of the frequency effect due to incident thermal fluxes at each temperature level.

Two problems with the CMP were discovered during pre-launch environmental testing. On three occasions, when all sensors were commanded to a specific temperature level, TQCM 2 went to the lowest temperatures it could attain. In each instance, this condition was corrected by individually commanding it to the specific temperature desired. This work-around seemed satisfactory. The second problem, involving noise in the controller for TQCM 3, caused the temperature of that crystal to oscillate as much as  $12^\circ\text{C}$  at times.

## Results

The STS-3 mission involved three major attitudes with respect to the sun for the purpose of verifying the Orbiter thermal design. These were tail-to-sun (TTS), with the Orbiter bay always facing away from both sun and the Earth; nose-to-sun (NTS), where the bay was not exposed to the sun and the roll rate allowed the Orbiter to view the Earth; and bay-to-sun (BTS), where the Orbiter bay faced the sun. The TTS attitude provided a very cold condition, NTS a moderately cold condition, and BTS a very hot condition. In the PTC attitude (also called the "barbecue mode"), the Orbiter rotated around its roll axis so that the sun could reach all surfaces. These conditions are reflected in temperatures measured by

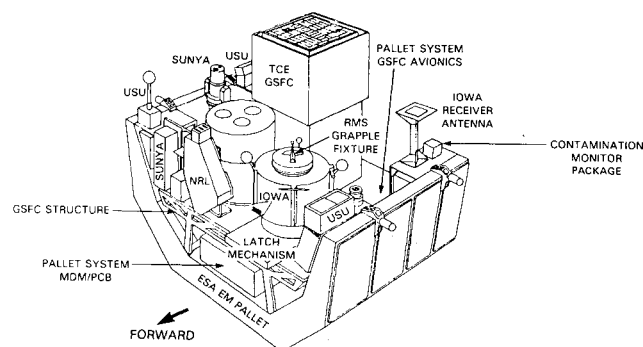


Fig. 1 OSS-1 pallet configuration.

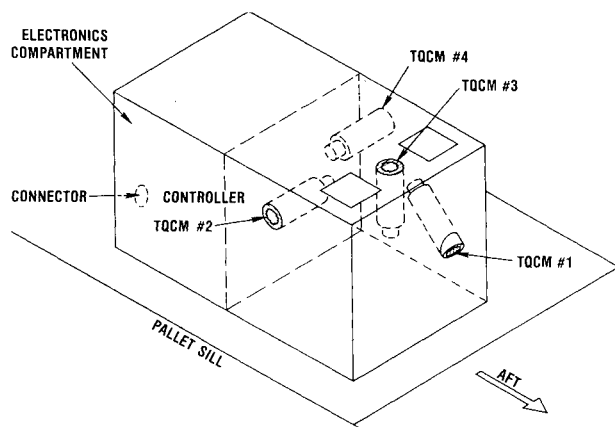


Fig. 2 Phantom view of Contamination Monitor Package (CMP).

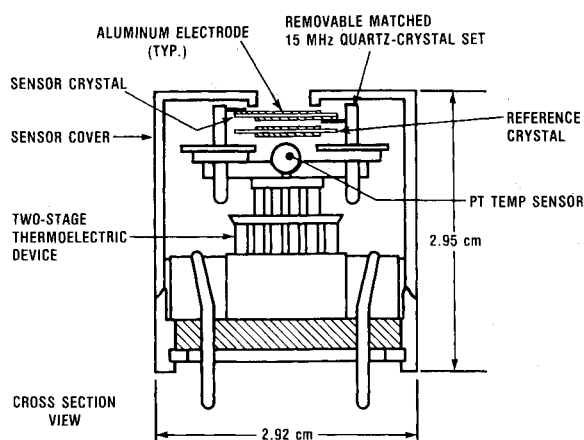


Fig. 3 TQCM sensor with thermoelectric device.

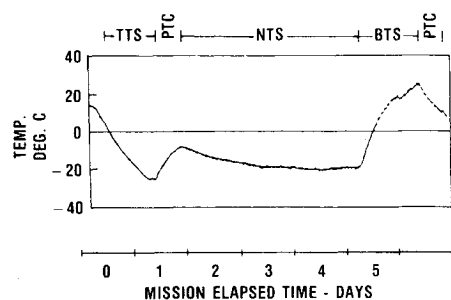


Fig. 4 OSS-1 pallet temperature as a function of mission elapsed time (MET).

OSS-1 thermistors, one of which (Fig. 4) was attached to the inner surface of a thermal blanket and one (Fig. 3) that was attached to a piece of equipment under the thermal blanket on the pallet.

For about the first day, while in the TTS orientation, the temperature dropped sharply. This was followed by a passive thermal control (PTC) mode that provided a more benign thermal environment as indicated by the rise in temperature in Fig. 4. This was then followed by about 3 1/4 days in the NTS attitude which resulted in a cool-down of the Orbiter bay and then a BTS condition for about a day which was accompanied by a pronounced warming trend. PTC, TTS, BTS, and other attitudes followed until deorbit. The importance of these temperatures is that they influenced the outgassing rates of the various materials and so influenced the measurements made by the CMP.

Figure 5 displays data from an OSS-1 pallet thermistor which measured the temperature of the low thermal mass, multilayer insulation. Here we can see wide fluctuations in rapid response to the various Orbiter orientations. These are more apparent in the expanded time-scale portion of the chart where the fluctuations with each orbit are better defined. Other temperature variations appear able to be correlated to other Orbiter maneuvers such as those for alignment of the Inertial Measurement Unit (IMU). Other temperature data exist for components with very high thermal inertia, and these show relatively small changes with Orbiter attitude. Since outgassing is a strong function of temperature, we expected to see significant differences with Orbiter attitude as indeed we did. However, since so many different temperatures and outgassing sources exist, one would expect to be able to predict only general trends. It is possible that in some cases, depletion of an outgassing source will occur while the temperature is increasing. These competing effects add to the uncertainty of predicting what will occur.

The TQCM data have been processed for the eight days of the mission. Time is expressed in terms of Mission Elapsed Time (MET), with the first three digits indicating the day, the next two the hours, the next two the minutes, and the last two the seconds. No data is available for the first few moments after liftoff. Following this period, data were gathered on the OSS-1 tape recorder using an "engineering format" that was incompatible with our automated data reduction technique. Data obtained during that period—lasting to about 000:01:45—were reduced by hand. No data were available from that point until about 000:03:30, when the OSS-1 experiments were activated. CMP data were then recorded in a "science format" that was compatible with our data reduction system. Nineteen short dropouts—a matter of a few minutes up to about 30 min—occurred during the remainder of the mission until the CMP was deactivated (006:22:15) prior to the planned landing. The CMP was turned on again in preparation for the planned landing on day 7 with the data being collected in the engineering format. Two longer data losses occurred, one from 001:23:15 to 002:05:20 and the other from 005:05:40 to 005:07:50.

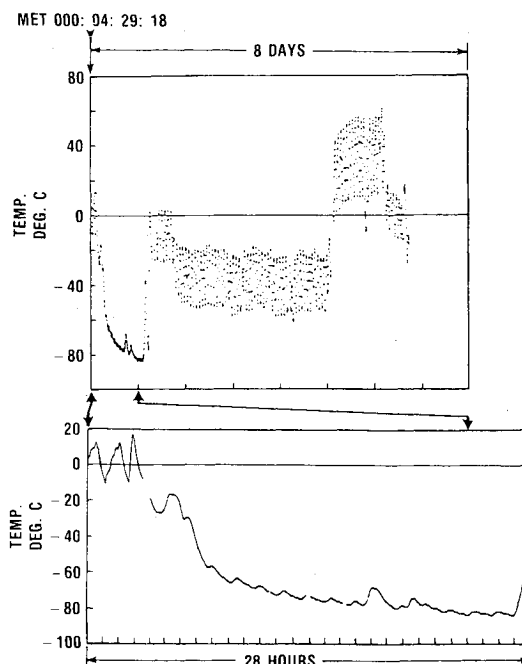


Fig. 5 Temperature of the outer layer of an OSS-1 thermal blanket as a function of MET.

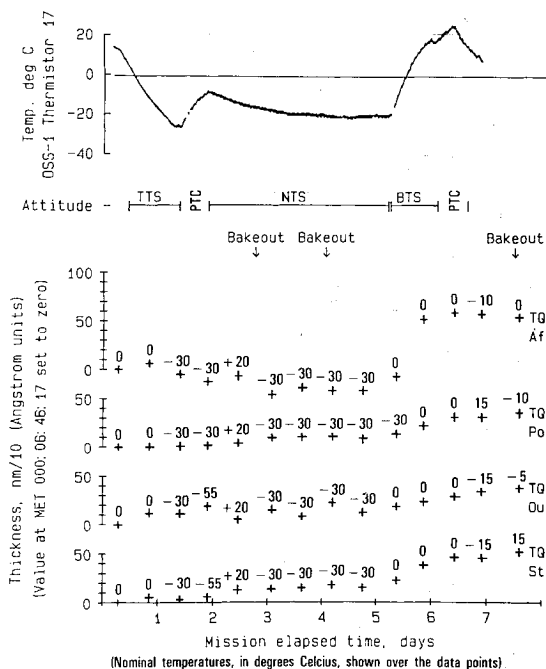


Fig. 6 Apparent contaminant thickness vs mission elapsed time.

With the delay of the landing until day 8, and concomitant extension of the mission, the capacity of the OSS-1 tape recorder was exceeded; it was turned off and then reactivated 2 1/2 h prior to landing. However, the CMP was active and data were downlinked when possible. This realtime data provided some continuity over the period when the OSS-1 tape recorder was not active. Before landing, sensor temperatures were set to +20, 0, and -10°C in an attempt to define the dew point on landing. Previous tests had shown that with a microbalance temperature below the dew point, one could expect it to saturate rapidly and stop oscillating when exposed to the water vapor. None of the TQCMs stopped functioning until they were turned off at about 008:00:15.

Table 1 Accretion rates indicated by the CMP during the STS-3 mission

MET		Orbiter attitude	TQCM temperature, °C	TQCM accretion rates, ng cm <sup>-2</sup> h <sup>-1</sup>			
from	to			1 (aft)	2 (port)	3 (out)	4 (stbd.)
000:12:50:16	000:15:50:25	TTS	+2	+4	+3	-2	+2
000:18:39:25	000:21:39:24	TTS	+1	+3	-1	-1	+3
001:01:00:30	001:04:00:38	TTS	-1	+3	0	-1	+3
001:05:15:19	001:06:45:42	TTS	-30	-2	0	+1	+5
001:06:45:42	001:08:15:27	TTS <sup>a</sup>	-30	-10	-8	+17	-2
001:12:45:22	001:15:45:29	PTC	-29	-9	+3	0	+3
002:06:30:07	002:09:30:18	NTS	+15	+7	-2	-13	+4
002:11:00:02	002:14:00:36	NTS	+14	-1	+4	+2	+2
003:02:00:23	003:03:30:08	NTS	-29	0	-12	-48	-2
003:04:45:38	003:07:45:43	NTS	-29	-2	-1	-9	-1
003:11:00:07	003:14:00:20	NTS	-29	-2	+1	+2	0
003:15:30:08	003:18:30:21	NTS	-29	+4	-1	+2	-2
004:03:00:05	004:06:00:15	NTS <sup>b</sup>	-29	-3	-13	+7	-12
004:13:20:00	004:16:20:08	NTS	-29	+1	0	+6	-2
005:00:05:07	005:03:05:05	NTS	-29	-3	+13	-4	-5
005:10:15:18	005:13:15:28	BTS	+1	+51	- <sup>c</sup>	+11	+32
005:15:00:17	005:18:00:30	BTS	+1	+81	+14	+2	+18
006:01:15:33	006:04:15:03	BTS	+17	+7	+12	+14	+9
006:05:45:28	006:08:45:22	BTS	+17	+26	+18	+16	+87 <sup>d</sup>
006:10:00:05	006:13:00:20	PTC	+1	-2	0	+2	-3

Notes: The values are based upon the differences between two groups of five points each either one or two orbits apart. The times given are the center points of the five. The temperatures can vary by 2°C from the value given; in the case of TQCM 3, instability often caused oscillations of as much as  $\pm 12^\circ\text{C}$ .

<sup>a</sup>Includes payload bay door opening and closing tests. <sup>b</sup>After a bakeout. <sup>c</sup>Temperature change took place during this period. <sup>d</sup>Temperature of TQCM 4 was  $-27^\circ\text{C}$ .

Table 2 Thickness differences between bakeouts

Time difference	Thickness difference, nm/10, (Angstrom units)		
	TQCM 1 T aft	TQCM 3 out	TQCM 4 stbd.
Day 2 to day 4	-5	-10	+7
Day 2 to day 7	+89	+40	+59

Although the sensor and reference crystals were matched to minimize the effect of temperature, some effect remained. Post-flight calibrations were conducted to define the effect of temperature on the TQCM frequency output, and appropriate corrections were made to TQCM frequency data to account for these calibrations.

In view of past data on similar devices (Refs. 3, 4, and others), it was decided that no calibration of mass vs frequency of the TQCM was needed.

Figure 6 presents the data in terms of thickness (using the assumption that the accreted material had a density of  $10\text{ g cm}^{-3}$ ). The data from Fig. 4 have been repeated in Fig. 6 to better portray the temperature effects. Data points are presented at approximately ten-orbit (16-h) intervals. The 10-orbit criterion was chosen so as to minimize the number of data points presented and thereby make Fig. 6 easier to read. The points at the beginning and end of each 10-orbit period were chosen to be shortly before the Orbiter passed from darkness into sunlight; this was done to eliminate the effects of solar flux and albedo on the TQCM output.

Detailed accretion rate information cannot be directly derived from the data on Fig. 6 because the data are presented at different temperatures and because events that can influence the readings take place between some of them. However, this is a striking increase in accretion from about day 5½ to day 6½; this corresponds to the BTS condition when outgassing would be expected to increase. (A complete presentation of the data will be made in a NASA document to be published at a later date.)

Other results of interest not included in Fig. 6 are as follows:

MET Day 0: Noticeable losses of mass were recorded between launch and some time after the payload bay doors were first opened (at MET day 0, approximately hour 2). This might have been due to the release of contaminants accumulated during the ground operations.

MET Day 3: At approximately 22:30 a special thruster firing, designated as an L2U burn, took place. (L2U is the designation for a particular Orbiter thruster firing.) All four TQCMs responded to this action.

MET Day 5: The TQCMs responded immediately when the Orbiter was reoriented to the BTS. Enhanced accretions continued even when the TQCM temperatures were raised to 0 and then  $+15^\circ\text{C}$ . TQCM 1, which faced aft and downward into the bay, recorded the greatest accretion rate.

MET Day 6: The Orbiter left the BTS orientation and accretion rates on all TQCM immediately dropped to low values. Toward the end of the day, the TQCMs were all set to different temperatures in preparation for the planned deorbit. However, because of landing site conditions, deorbit was delayed for one day.

Table 1 presents accretion rates for a number of periods during the mission.

The results of the three bakeouts conducted on days 2, 4, and 7 are shown in Table 2. The differences in the thickness indicated by the TQCMs after a period at  $+60^\circ\text{C}$  between days 2 and 4 show two at a lower thickness on the later date and one with an increase of 7 nm/10 (Angstrom units). However, the second line shows that, even with bakeout, there was a net increase of 40 to 89 nm/10 (Angstrom units) between days 4 and 7. This includes the period when the Orbiter was in the BTS orientation. (TQCM 2 data are not presented because the temperature was not at  $+60^\circ\text{C}$  during bakeouts on days 4 and 7).

## Conclusions

The accretions recorded by TQCMs throughout the mission followed a predictable pattern based on the temperature profile of the payload and its surroundings. Very few Orbiter

events had an effect on the instrument responses. Our experiences with this instrument showed the feasibility and advantages of a small realtime contamination monitor that can be controlled from the ground and is compatible with almost any cargo mix.

#### Acknowledgments

The authors would like to acknowledge the assistance of Lt. E. Christ (SD) and Ms. A. Phillips (JPL) during the mission operations.

#### References

<sup>1</sup>Miller, E.R. and Decher, R., "An Induced Environment Con-

tamination Monitor for the Space Shuttle," NASA TM-78193, Aug. 1978.

<sup>2</sup>Scialdone, J.J., "Assessment of Shuttle Payload Gaseous Environment," NASA TM-80286, May 1979.

<sup>3</sup>McKeown, D. and Corbin, W.E., "Thermoelectrically-Cooled Quartz Crystal Microbalance," *Seventh Conference on Space Simulations*, NASA SP-336, 1973.

<sup>4</sup>McKeown, D. and Corbin, W.E. Jr., "Space Measurements of the Contaminants of Surfaces by OGO-6 Outgassing and Their Cleaning by Sputtering and Desorption," *Space Simulation*, U.S. Department of Commerce, National Bureau of Standards, Special Pub. 336, Oct. 1970.

## *From the AIAA Progress in Astronautics and Aeronautics Series . . .*

### **SATELLITE COMMUNICATIONS:**

#### **FUTURE SYSTEMS-v. 54**

#### **ADVANCED TECHNOLOGIES-v. 55**

*Edited by David Jarett, TRW, Inc.*

Volume 54 and its companion Volume 55, provide a comprehensive treatment of the satellite communication systems that are expected to be operational in the 1980's and of the technologies that will make these new systems possible. Cost effectiveness is emphasized in each volume, along with the technical content.

**Volume 54** on future systems contains authoritative papers on future communication satellite systems in each of the following four classes: North American Domestic Systems, Intelsat Systems, National and Regional Systems, and Defense Systems. **A significant part of the material has never been published before.** Volume 54 also contains a comprehensive chapter on launch vehicles and facilities, from present-day expendable launch vehicles through the still developing Space Shuttle and the Intermediate Upper Stage, and on to alternative space transportation systems for geostationary payloads. All of these present options and choices for the communications satellite engineer. The last chapter in Volume 54 contains a number of papers dealing with advanced system concepts, again treating topics either not previously published or extensions of previously published works.

**Volume 55** on advanced technologies presents a series of new and relevant papers on advanced spacecraft engineering mechanics, representing advances in the state of the art. It includes new and improved spacecraft attitude control subsystems, spacecraft electrical power, propulsion subsystems, spacecraft antennas, spacecraft RF subsystems, and new earth station technologies. Other topics are the relatively unappreciated effects of high-frequency wind gusts on earth station antenna tracking performance, multiple-beam antennas for higher frequency bands, and automatic compensation of cross-polarization coupling in satellite communication systems.

With the exception of the first "visionary" paper in Volume 54, all of these papers were selected from the 1976 AIAA/CASI 6th Communication Satellite Systems Conference held in Montreal, Canada, in April 1976, and were revised and updated to fit the theme of communication satellites for the 1980's. These archive volumes should form a valuable addition to a communication engineer's active library.

*Volume 54, 541 pp., 6 x 9, illus., \$19.00 Mem., \$35.00 List*  
*Volume 55, 489 pp., 6 x 9, illus., \$19.00 Mem., \$35.00 List*  
*Two-Volume Set (Vols. 54 and 55), \$38.00 Mem., \$55.00 List*

TO ORDER WRITE: Publications Order Dept., AIAA, 1633 Broadway, New York, N.Y. 10019